Metagenomic insights into nitrification and urease inhibitors promote glyphosate degradations and reduce soil nitrous oxide emissions

Yaohui Liu

Jiangxi Provincial Key Laboratory of Silviculture, College of Forestry, Jiangxi Agricultural University, Nanchang 330045, China

Abstract

Organic herbicide pollution and greenhouse gas emission are major concerns in achieving sustainable agriculture and forestry. Nitrification and urease inhibitors have been used to improve fertilizer nitrogen (N) use efficiency, but their interactions with herbicides have rarely been studied. A comprehensive understanding of the impacts of N-cycling inhibitors on pesticide degradation and nitrous oxide (N_2O) emission could help minimize the environmental risks of herbicide pollution and global climate change. In this study, we investigated glyphosate residues and N_2O emission in camellia plantation soils, as influenced by nitrification inhibitors 3,4-dimethyl pyrazole phosphate (DMPP) and dicyandiamide (DCD) and urease inhibitor thiophosphoric triamide (NBPT), under 60% and 90% water holding capacity (WHC). The soil properties, glyphosate residues, N_2O emissions, microbial communities and their comprehensive linkages were also analyzed. Compared with the control treatment, applying DMPP, DCD and NBPT significantly decreased glyphosate residues by 32.9%, 60.3% and 35.6% under 90% WHC, respectively. Soil glyphosate residues were negatively correlated to the abundances of *Acidobacteria* and *phn*X gene. Contributions of soil moisture to glyphosate degradation were correlated to increases in *phn*J, *sox*A and *sox*D genes. Relative to the control treatment, NBPT applications decreased cumulative N_2O emissions by 56.6% and 91.4% under 60% and 90% WHC, respectively. Soil N_2O emissions were regulated by soil water contents partly through affecting changes in soil DOC, DON, NH_4^+-N and NO_3^--N contents as well as abundances of functional *nos*Z, *nar*G, *nor*B and *nor*H genes. The promotion of glyphosate degradation and suppression of soil N_2O emission by the N-cycling inhibitors suggested that applying N-cycling inhibitors might be an effect strategy to simultaneously reduce environmental pollution of pesticides and global climate change.

1. Introduction

Herbicides and nitrogen (N) fertilizers are commonly used for improving crop productivity. Glyphosate (*N*-phosphonometylglycine) is an effective herbicide that is widely applied for suppressing weed growth[1, 2]. However, over-application of glyphosate can lead to substantially adverse impacts including soil pollution and microbial activity inhibition.[2, 3] Meanwhile, the glyphosate can stimulate soil denitrification and accelerate greenhouse gas emission.[4, 5] The degradation of glyphosate is affected by soil properties, microbial activity and functional genes.[1, 6-9] In addition, soil N managements could also affect agrochemical transformations and translocations in soil-plant systems; for instance, a previous study confirmed that N-cycling inhibitors could accelerate carbendazim degradation by affecting functional microbes.[10]

Fertilizer N usually has inefficient utilization due to processes like nitrification, nitrate (NO_3^--N), leaching and denitrification.[11, 12] Nitrification is a vital process in which ammonium nitrogen (NH_4^+-N) is converted to NO_3^--N that is the substrate of denitrification, a major pathway for nitrous oxide (N_2O) emissions.[13-15] N_2O is a potent greenhouse gas with 273 times greater global warming potential than carbon dioxide over a 100-year time.[16, 17] Applying nitrification or urease inhibitors is an effective practice for reducing N_2O emissions and improving N

utilization efficiency via slowing nitrification or denitrification, urea hydrolysis.[18] Nitrification inhibitors 3,4-dimethyl pyrazole phosphate (DMPP) and dicyandiamide (DCD) and urease inhibitor thiophosphoric triamide (NBPT) are the main commercial N-cycling inhibitors and are widely applied to inhibit nitrification and decrease soil N_2O emissions.[19-21] The N-cycling inhibitors might also modify the dissipation rates of agrochemicals. [10] However, the effects of N-cycling inhibitors on glyphosate degradation and the related functional mechanisms were rarely studied.

Soil moisture substantially affects N-cycling genes, N_2O emissions and microbial communities.[22-24] For example, studies suggested that increasing water holding capacity (WHC) from 60% to 120% significantly increased soil N_2O emissions by stimulating *nir*S genes.[25] Liu et al. proposed that soil moisture regulates N_2O emissions via influencing N-cycling related genes expression and microbiological activity.[26] Nonetheless, how variation in soil moisture modifies the impacts of N-cycling inhibitors on agrochemical dissipation and the related functional mechanisms are unknown.

A comprehensive understanding of the impacts of N-cycling inhibitors on herbicide dissipation and N_2O emission will help to simultaneously deal with the environmental risks of organic pollution and global climate change. Thereby, this study investigated the effects of the N-cycling inhibitors on soil glyphosate degradation and N_2O emission reduction and deciphered the comprehensive linkages among the functional genes and microorganisms, glyphosate residues and N_2O emissions under different soil moistures. Soil samples were collected from a camellia plantation with long-term (7 years) glyphosate applications. The DMPP, DCD and NBPT were applied to the test soil, and then soil properties, N_2O emission, glyphosate residues and microbial metagenomics were analyzed. This study aimed to: (1) quantify the impacts of N-cycling inhibitors on both soil glyphosate degradation and N_2O emissions reduction under various moistures; (2) identify the functional microbes and genes associated with glyphosate degradation and N_2O emissions; and (3) decipher the major mechanisms of N-cycling inhibitors affecting glyphosate degradation under the different soil water contents. The results will help better understand benefits of N-cycling inhibitor utilization and provide technical support to decrease the risks of glyphosate pollution and mitigating greenhouse gas emissions.

2. Materials and methods

2.1 Soil sampling and experimental design

Experimental soil (0-20 cm) was collected from an intensively managed camellia plantation in Jiangxi, China (27°74′ N, 114°81′ E). The site had received long-term (7 years) glyphosate application (15 kg ha^{-2} y^{-1}). The collected soil was passed through a 2 mm sieve to remove stones and litter, and stored at -20 °C until used. Soil chemical properties were given in Table S1, and the glyphosate content was190.74 mg kg^{-1} dry soil.

The experimental design contained 4 different treatments: blank control (CK), DMPP application (DMP), DCD application (DCP) and NBPT application (NBP) under two different soil water contents (60% and 90% WHC). Each treatment was replicated 4 times. Fresh and sieved soil samples (equivalent to 40 g dried soil) were placed in 200 mL conical flasks, and each sample received 8 mg N as urea. The N-cycling inhibitors were applied at 1% of the urea N. The urea and N-cycling inhibitors were dissolved in deionized water and then added into the flasks and thoroughly mixed. Soil moistures were separately adjusted to 60% and 90%WHC, before the microcosms were incubated at 25 °C in the dark. The moistures were maintained by adding deionized water every day. Soil N_2O emission rates were quantified on 0.5, 1, 4, 7, 14, and 28 days. Soil properties, glyphosate residues and microbial metagenomic were analyzed at the end of the experiment.

2.2 Determination of soil glyphosate residue

Soil glyphosate residues were extracted and then analyzed using an ultra-performance liquid chromatography.[28] In brief, test soils were freeze-dried and ground to < 0.25 mm. Approximately 5.0 g of the samples were added into a 50 mL flask containing 25 mL of the extraction solution of sodium phosphate and sodium citrate, shaken and filtered through filter paper. The filtered solutions were mixed with boric acid and 9-fluorenylmethoxycarbonyl chloride solution and allowed to stand for 4 h before centrifuged and filtered through 0.22 μm filters for quantitative glyphosate analysis by an ultra-performance liquid chromatography. The injection volume was 20.0 μL, and the flow rate was 1 mL min^{-1} with mobile phase A (acetonitrile solution) and B (phosphoric acid solution) in the C_{18} chromatographic column. The glyphosate was identified by matching the peak area of the glyphosate standard and quantified with an external glyphosate standard curve.

2.3 N_2O sampling and analysis

The gas was sampled and analyzed according to the method of Zheng et al [29] with minor modifications. Briefly, an air blower was used to refresh the gas in the flask headspace before sampling, and each flask was immediately sealed using a rubber stopper installed with a three-way stopcock. Plastic syringes were employed to collect initial and final gas samples from the headspace of the sealed flasks during each 3 h incubation period. The N_2O concentrations were analyzed by a gas chromatograph (Agilent 7890B, Santa Clara, CA, USA).

2.4 Determinations of soil chemical properties

Soil pH was determined using an electronic pH meter. Soil dissolved organic carbon (DOC) and N (DON) were determined by a Total Organic C/N Analyzer (Multi N/C 2100, Germany). Soil NH_4^+-N and NO_3^--N were quantitatively analyzed by the Discrete Auto Analyzer (SmartChem, Brookfield, France). Soil available phosphorus (AP) contents were measured using the molybdenum antimony colorimetric method.

2.5 Soil DNA extraction and metagenomic sequencing

Total DNA in each fresh sample was extracted for metagenomic sequencing. The NDA extractions, PCR amplification, and sequencing were conducted according to the guidance by Novogene (Beijing, China) and the raw data was submitted to the NCBI database (PRJNA977811). Basic information on the metagenomic sequencings was provided in Table S2. Soil microbial information was obtained through blasting with the Non-Redundant Protein Sequence Database (NR) database, and the Kyoto Encyclopedia of Genes and Genomes (KEGG) database was used for N transformation and glyphosate degradation gene annotations. The genes related to glyphosate degradation were selected and shown in Table S3, and key functional genes related to N transformation were given in Tables S4. The relative abundances of selected functional genes were normalized to 10^4 cells after dividing the abundance of the housekeeping gene *rpl*B for further statistical analysis.[30]

2.6 Statistical analysis

Two-way analysis of variance (ANOVA) was employed to evaluate the interactions between the N-cycling inhibitors and soil water contents on soil abiotic and biotic characters. One-way ANOVA was carried out to assess the impacts of different treatments on soil chemical properties, glyphosate residues, N-cycling and glyphosate degradation related genes, and soil microbial community diversities with Duncan's multiple range test using the SPSS 26.0 (IBM, USA). The principal component analyses (PCA) were conducted to reveal the differences in soil microbial community structures. The first principal component of the soil chemical properties, microbial community structures, and functional genes related to N-cycling or glyphosate degradation were extracted for further quantitative analysis. Pathway analyses were constructed to elucidate the comprehensive linkages among soil chemical properties, glyphosate residues, functional genes related to N-cycling and glyphosate degradation, and microbial communities using the SPSS Amos 26.0 (IBM, USA).

3. Results

3.1 Soil glyphosate residues

Negligible changes in soil glyphosate residues were detected among the four treatments under 60% WHC (Fig.1a). However, under 90% WHC, soil glyphosate residues in the DMPP, DCP and NBP treatments significantly decreased by 33.0%, 60.3% and 35.7%, relative to the CK treatment (184.52 mg kg^{-1}), with the lowest glyphosate residue detected in the DCP treatment (73.17 ± 6.17 mg kg^{-1}). Significant differences in glyphosate residues in the DMP, DCP and BNP treatments were also detected between 60% and 90% WHC.

3.2 Soil N_2O emissions

Relative to the CK treatment, N_2O emissions were inhibited in the DMP treatment after the first day under 60% and 90% WHC (Fig. S1). Soil N_2O emission rates at the end of experiment had the order of CK＞DMP＞DCP＞NBP under 60% WHC. While, the N_2O emission rates on day 28 in the CK, DMP, DCP and NBP treatments were 0.5261, 0.4020, 0.48323 and 0.0046 ng N g^{-1} dry soil h^{-1} respectively, under 90% WHC.

Under 60% WHC, soil cumulative N_2O emissions were in the order of CK > DMP > DCP > NBP, being 0.043 ± 0.00, 0.031 ± 0.120, 0.025 ± 0.000 and 0.019 ± 0.000 μg g^{-1} dry soil, respectively, and the DCP and BNP treatments had significantly lower cumulative N_2O emission than that in the CK treatment (Fig.1b). In comparison with the CK treatment, soil cumulative N_2O emissions in the DCP and DMP treatments decreased by 30.46% and 91.48% under 90% WHC, respectively.

3.3 Soil chemical properties

Relative to those under 60% WHC, significantly higher pH values were observed among all soil samples under 90% WHC (Table 1). Relative to the CK treatment, soil DOC contents in the DCP and NBP treatments increased by 72.83% and 64.31%, respectively, under 60% WHC, but neglectable differences in DOC contents were found among the four treatments under 90% WHC. Although soil DON contents decreased in the order of NBP > DCP > DMP > CK under 60% WHC, the contrary order of DON contents were detected under 90% WHC (CK > DMP > DCP > NBP). Further, higher DON contents in the DMP, DCP and NBP treatments were observed under 60% WHC than their counterparts under 90% WHC, and the treatment and soil water content had significantly interactive effects on DON contents (Table S5). Although no significant differences in NH_4^+-N contents were observed across the four treatments under 60% WHC, soil NH_4^+-N contents in the DMP, DCP and DMP treatments were significantly lower than those in the CK treatment under 90% WHC. Moreover, 60%NH_4^+-N contents were higher among all soil samples under 60% WHC than their counterparts under 90% WHC. Relative to the CK counterparts, soil NO_3^--N contents reduced by 59%, 15% and 63% in the DCP, DMP and NBP treatments under 60% WHC and decreased by 73% and 55% and 93% in the DCP, DMP and NBP treatments under 90% WHC, respectively. Soil NO_3^--N contents in all samples 90%were significantly lower under 90% WHC than under 60% WHC. The soil AP contents in the DMP treatment were significantly lower than those in the CK treatment under 60% WHC, but no significant differences in AP contents were observed across the four treatments under 90% WHC.

3.4 Functional microbes and genes associated with glyphosate degradation

Relative to the CK treatment, the other treatments had no significant changes in the normalized abundances of *phn*G, *phn*H, *phn*I, *phn*J, *phn*X and *phn*P genes encoding C-P lyase under 60% WHC, but the abundances of the *phn*I gene in the DCP and DMP treatments and the *phn*X gene in the DCP treatment were significantly higher under 90% WHC (Figs. 2a-f). There were no significant changes in abundances of biodegradation gene *sox*A, *sox*D and *sox*G across the different treatments (Figs. 2g-i). Relative to the CK treatment, the BNP treatment had lower *aro*E gene abundance under 60% WHC, but *aro*E gene abundances were higher in the DCP and NBP treatments under

60% WHC (Figs. 2j and k). The NBP treatment had higher *aro*E gene abundance than its counterparts in the CK treatment under 90% WHC.

3.5 Functional microbes and genes associated with soil N-cycling

The functional genes related to N-cycling were shown in Fig. 3. Although no significant differences in *nir*B and *nir*D genes abundances were observed among the treatments under 60% WHC, significant decreases in these gene abundances were shown in the DCP treatment under 90% WHC (Figs. 3a and b). Significant increases in the *nar*B and *nar*J/W genes normalized abundances were also found, but contrary effects on the *hao* gene were detected in the NBP treatment between 60% and 90% WHC (Figs. 3c-e). The normalized abundance of *amo*C gene in the DMP treatment under 90% WHC was 4.03 times higher than that under 60% WHC (Fig. 3f). Under 90% WHC, significant decreases in the *nar*G gene were shown in the DMP treatment, and significant decreases in *nar*B gene abundances were found in the DMP and DCP treatments (Figs. 3g and h). Although neglectable differences in the denitrifying *nap*A, *nar*H, *nap*B, and *nos*Z genes were found across the treatments under 90% WHC, significant differences (except the *nap*A gene) in the DCP treatment were detected between 60% WHC and 90% WHC (Figs. 3i-l). There were negligible changes in the *gdh*A, *gdh*B, *ure*C, *nif*K and *nif*U genes among the four different treatments under 60% WHC, but they were significantly different across the four treatments under 90% WHC, with significant increases in *gdh*A and *nif*U gene abundances in the NBP treatment (Figs. 3m-q). The bubble diagram revealed the relationships between soil microbes and N-cycling related genes; the denitrification gene of *nir*D was mainly encoded by the *Firmicutes*, *Acidobacteria* and *Tectomicrobia* (Fig. S3b).

3.7 Microbial community diversities and structures

The *Proteobacteria* and *Acidobacteria* were the two dominant microbes, being 35.57%-46.66% and 35.71%-45.47%, respectively (Figs. S4a and b). The relative abundances of *Proteobacteria* in the DCP and NBP treatment significantly decreased, but *Acidobacteria* relative abundances significantly increased in the DCP treatment compared with the CK treatment under 90% WHC (Figs. S4c and d). Relative to the CK treatment, no significant changes in *Actinobacteria* and *Verrucomicrobia* relative abundances were detected in the DMP, DCP and NBP treatments (Figs. S4e and f). The *Chloroflexi* relative abundance significantly increased by 15.58% in the DCP treatment, in comparison with the CK treatment under 90% WHC (Fig. S4g). The NBP treatment had higher the *Planctomycetes* relative abundances under both 60% and 90% WHC, relative to the CK counterparts (Fig. S4h). Compared to the CK treatment, *Gemmatimonadetes* relative abundance was significantly higher in the BNP treatment and was significantly affected by soil moistures (Fig. S4i), and higher relative abundances of *Rokubacteria* and *Bacteroidetes* were detected in the NBP treatment under different moistures (Fig. S4k). There were no significant differences in *Eremiobacteraeota* relative abundances among the four treatments under 60% WHC or 90% WHC (Fig. S4l). The relative abundances of *Cyanobacteria* were substantially inhibited in the DMP and NBP treatments, relative to the CK treatment under 60% WHC (Fig. S4m). The *Firmicutes* relative abundance in the NBP treatment was significantly increased, relative to the CK treatment under 60% and 90% WHC (Fig. S4n). No biomarkers were found in the NBP treatment under 60% WHC, but the *Bradyrhizobium guangzhouense* was the main biomarker of soil microbes in the NBP treatment under 90% WHC (Figs. S2a and b).

The axis 1 and axis 2 accounted for 46.77% and 53.14% of the total variations of soil microbes under 60% WHC and 90% WHC, respectively (Figs. 4a and b). Although no significant changes in microbial community structures were detected among all treatments under 60% WHC, significant separations were shown between the NBP treatment and other treatments under 90% WHC. Soil glyphosate residues had negative influences on soil microbial community structures in the NBP treatment.

3.8 Factors influencing soil glyphosate residue and N_2O emissions

Glyphosate residues were not significantly correlated to soil chemical properties but negatively related to the abundances of *aro*A gene and the relative abundances of *Planctomycetes*, *Firmicutes*, *Tecomicrobia*, *Rokubacteria* and *Acidobacteria* under 60% WHC (Fig. 5c). Under 90% WHC, glyphosate residues had positive correlations to soil DON, NH_4^+-N and NO_3^--N but were negatively related to *phn*X gene and *Acidobacteria* relative abundances (Fig. 5d). Under both 60% and 90% WHC, glyphosate residues had negative correlations with the *Acidobacteria* relative abundances but were positively associated with the *Proteobacteria* relative abundances.

Soil N_2O emissions at the end of experiment was negatively related to DOC and DON under 60% WHC, and pH under 90% WHC, but positive relationships were observed between N_2O emission rate and NO_3^--N under both 60% and 90% WHC (Figs. 4c and d). Soil N_2O emission rate had positive correlations to functional *nar*G and *anr*H genes but was negatively related to the relative abundances of *Eremiobacteraeota*, *Chloroflexi*, *Firmicutes* and *Nitrospirae* under 60% WHC. Under 90% WHC, N_2O emission rates were correlated positively to *amo*C gene abundances, but negatively to the abundances of *gdh*A and *nif*U genes and the relative abundances of *Armiatimonadetes*, *Eremiobacteraeota*, *Tectomicrobia*, *Chrysiogenetes*, *Firmicutes* and *Nitrospirae*.

Pathway analysis revealed positive correlations between glyphosate residues and glyphosate degradation related genes (Fig. 6). Soil property changes in pH, DOC, DON NH_4^+-N and NO_3^--N associated with the N-cycling inhibitor applications not only stimulated soil glyphosate decline but also reshaped microbial community structures, and microbial community structures had positive correlations to glyphosate-degrading genes.

4. Discussion

4.1 Glyphosate degradation and functional microbes and genes

Applying N-cycling inhibitors significantly decreased soil glyphosate residues and altered functional gene abundances, with greater effects under 90% WHC than 60% WHC (Fig. 1a). The increases in glyphosate degradation were related to changes in soil chemical and microbial properties following N-cycling inhibitor applications: (1) the positive effects of soil DOC, DON and NH_4^+-N to glyphosate degradation were observed,[31] (2) *Acidobacteria* could degrade different agrochemicals including glyphosate, and increases in the relative abundances of *Acidobacteria* could promote the glyphosate dissipations in soils;[32] (3) the *phn*X gene encodes C-P lyase responsible for glyphosate degradation,[32] and thus increases in *phn*X gene in the DCP treatment under 90% WHC might degrade glyphosate via breaking the C-P bond (Figs. 1 and 2). This was supported by the negative correlation between glyphosate residue and the *phn*X gene under 90% WHC (Fig. 5d).

Soil water content is a vital factor affecting degradation of glyphosate residues, although glyphosate has high solubility.[33, 34] Negative correlation between decreased glyphosate residues and *Acidobacteria* was only observed under 90% WHC (Fig. 5). *Acidobacteria* could degrade glyphosate according to Rossi et al.[32] *Chloroflexi* could also contribute to soil glyphosate degradation.[35] It can be inferred that increases in *Chloroflexi* in the DCP treatment under 90% WHC might have contributed to the glyphosate degradation in this study (Fig. 5). Further, *Chloroflexi* acodes *phn*H gene, which can code C-P lyase for glyphosate degradation (Fig. S3). Both *phn*H and *phn*J genes encoding C-P lyase and *sox*A gene encoding sarcosine oxidase significantly increased in the DMP treatment (Fig. 2), implying that those functional genes might have participated in the degradation of glyphosate.[8] Increases in *sox*D gene in the DMP treatment under 90% WHC might also contribute to degradation of glyphosate (Fig.2). The degradation of glyphosate produces sarcosine, which could stimulate *sox*A and *sox*D genes for encoding sarcosine oxidase.

4.2 Soil N-cycling and the corresponding microbes and genes

Nitrification inhibitors decreases nitrification and soil NO_3^--N production, but significant decreases in soil NH_4^+-N contents were observed under 90% WHC (Table 1). The results were contrary to findings that N-cycling inhibitors increased or maintained soil NH_4^+-N contents.[10, 36] The reason might be that soil moisture can affect the efficacy of N-cycling inhibitors. Some studies suggested that the efficacy of DMPP for nitrification inhibition could be lost when soil water content was over 60% of water-filled pore space.[37, 38] Puttanna et al. (1999) also reported that the nitrification inhibitors were less effective under 80% WHC than 40% and 60% WHC. [27]

The N-cycling inhibitors decreased cumulative N_2O emissions more effectively under 90% WHC, relative to 60% WHC (Fig. 1b). These results were supported by other studies.[21, 39] On one hand, nitrification inhibitors could inhibit the production of NO_3^--N and indirectly reduce the substrate concentration for denitrification, leading to N_2O emission reduction.[40, 41] On the other hand, soil N_2O emission was positively correlated with soil water content because high soil water content could decrease oxygen gas availability but stimulate the denitrification process to emit more N_2O.[25, 42, 43]

Functional mechanisms driving soil N_2O emissions were different under various soil water contents (Figs. 5c and d). Soil N_2O emission rates were positively related to NO_3^--N but negatively correlated to soil pH, DOC and DON, and the special microbes and functional genes under both soil water contents. The reasons for these relationships might be (1) soil NO_3^--N was the primary substance for producing N_2O by denitrification;[44, 45] (2) high DON contents implied that more urea N was immobilized in soil organic matter, which were not immediately available as substrate for N_2O production;[46] (3) Soil microbes, especially nitrifiers and denitrifiers, play vital roles in soil N_2O production and emission.[47, 48] In our current study, soil N_2O emission rates were negatively related to the relative abundances of *Firmicutes, Chrysiogenetes, Tectomicrobia*, *Chloroflexi* and *Nitrospirae* (Fig. 5), and it has been confirmed that those microbes were closely involved in N transformations in soils [49-53]; (4) the *nar*G and *nar*H genes involved in the denitrification process were inhibited by N-cycling inhibitors application, decreasing N_2O emission under 90% WHC (Figs. 3 and 6). Moreover, increases in denitrifying *nos*Z, *nar*G, *nar*H and *nar*B gene abundances in varying degrees might also stimulate soil denitrification for N_2O production, thus higher N_2O emissions under 90% WHC than that under 60% WHC.[48]

Declaration of competing interest

The authors declare that they have no known competing financial interests.

Author contributions

Yaohui Liu, and Manyun Zhang designed the study, analyzed the data, and drafted the manuscript. Yaohui Liu, Haoqi Fan and Kewei Ren collected the data. Manyun Zhang, Weijin Wang, Negar Omidvar, and Dongnan Hu interpreted the results and revised the manuscript and data presentation.

Acknowledgments

This research was supported by the National Natural Science Foundation of China (31560218) and the National Key Research and Development Program (2018YFD1000603) by Dongnan Hu.

References

(1) Allegrini, M.; Gomez, E. V.; Zabaloy, M. C. Repeated glyphosate exposure induces shifts in nitrifying communities and metabolism of phenylpropanoids. *Soil Biol. Biochem.* **2017**, *105*, 206-215.

(2) Tush, D., Meyer, M. T. (2016). Polyoxyethylene tallow amine, a glyphosate formulation adjuvant: soil adsorption characteristics, degradation profile, and occurrence on selected soils from agricultural fields in Iowa, Illinois, Indiana, Kansas, Mississippi, and Missouri. *Environ. Sci. Technol.* **2016**, *50*, 5781-5789.

(3) Zanin, A. R. A.; Neves, D. C.; Teodoro, L, P, R.; Júnior, C. A. S.; Silva, S. P.; Teodoro, P. E.; Baio, F. H. R. Reduction of pesticide application via real time precision spraying. *Sci. REP-UK* **2022**, *12*, 5638.

(4) Stratton G. W.; Stewart, K. E. Effects of the herbicide glyphosate on nitrogen cycling in an acid forest soil. *Water, Air, Soil Poll.* **1991**, *60*, 231-247.

(5) Yang, X.; Bento, C. P. M.; Chen, H.; Zhang, H.; Xue, S.; Lwanga, E. H.; Zomer, P.; Ritsema, C. J.; Geissen, V. Influence of microplastic addition on glyphosate decay and soil microbial activities in Chinese loess soil. *Environ. Pollut.* **2018**, *242*, 338-347.

(6) Aslam, S.; Jing, Y.; Nowak, K. M. Fate of glyphosate and its degradation products AMPA, glycine and sarcosine in an agricultural soil: Implications for environmental risk assessment. *J. Hazrd. Mater.* **2023**, *477*, 130847.

(7) Schnürer, Y.; Persson, P.; Nilsson, M.; Nordgren, A.; Giesler, R. Effects of surface sorption on microbial degradation of glyphosate. *Environ. Sci. Technol.* **2006**, *40*, 4145-4150.

Cecilia, D., Maggi, F. Analysis of glyphosate degradation in a soil microcosm. *Environ. Pollut.* **2018**, *233*, 201-207.

(8) Wilms, W., Parus, A.; Homa, J.; Batycka, M.; Niemczak, M.; Wo´zniak-Karczewska, M.; Trzebny, A.; Zembrzuska; Dabert, M.; Tancsics, A.; Cajthaml, T.; Heipieper, H. J.; Chrzanowski, Ł. Glyphosate *versus* glyphosate based ionic liquids: Effect of cation on glyphosate biodegradation, *sox*A and *phn*J genes abundance and microbial populations changes during soil bioaugmentation. *Chemosphere* **2023**, *316*, 137717.

(9) Muskus, A. M.; Miltner, A.; Hamer, U.; Nowak, K. M. Microbial community composition and glyphosate degraders of two soils under the influence of temperature, total organic carbon and pH. *Environ. Pollut.* **2022**, *297*, 118790.

(10) Guo, T.; O'Connor, P. J.; Zhao, X.; Zhou, T.; Wang, Y.; Zhang, M. The win-win effects of nitrification inhibitors on soil-crop systems: decreasing carbendazim residues but promoting soil bacterial community diversities and stabilities and crop yields. *J. Hazrd. Mater.* **2023**, *451*, 131175.

(11) Mason, R. E.; Craine, J. M.; Lany, N. K.; Jonard, M.; Ollinger, S. V.; Groffman, P. M.; Fulweiler, R. W.; Angerer, J.; Read, Q. D.; Reich, P. B.; Templer, P. H.; Elmore, A. J. Evidence, causes, and consequences of declining nitrogen availability in terrestrial ecosystems. *Science* **2022**, *376*, 261.

(12) Duan, P.; Yang, X.; He, X.; Jiang, Y.; Xiao, K.; Wang, K.; Li, D. Topography‐driven soil properties modulate effects of nitrogen deposition on soil nitrous oxide sources in a subtropical forest. *Biol. Fertil. Soils* **2022**, *58*, 707-720.

(13) Duan, P.; Xiao, K.; Jiang, Y.; Li, D. Mechanisms underlying the responses of soil N_2O production by ammonia oxidizers to nitrogen addition are mediated by topography in a subtropical forest. *Geoderma* **2022**, *425*, 116036.

(14) Woodward, E. E.; Edwards, T. M.; Givens, C. E.; Kolpin, D. W.; Hladik, M. L. Widespread use of the nitrification inhibitor nitrapyrin: assessing benefits and costs to agriculture, ecosystems, and environmental health. *Environ. Sci. Technol.* **2021**, *55*, 1345-1353.

(15) Meng, Y.; Wang, J., Wei, Z.; Dodla, S. K.; Fultz, L. M.; Gaston, L. A.; Xiao, R.; Park, J.; Scaglia, G. Nitrification inhibitors reduce nitrogen losses and improve soil health in a subtropical pastureland. *Geoderma* **2021**, *388*, 114947

(16) Ravishankara, A. R.; Daniel, J. S.; Portmann, R. W. Nitrous oxide (N_2O): the dominant ozone-depleting substance emitted in the 21st century. *Science* **2009**, *326*, 123-125.

(17) IPCC, 2021. Climate change 2021: the physical science basis. In: Masson-Delmotte, V., Zhai, P., Pirani, A., Connors, S. L., Pean, C., Chen, Y., Goldfarb, L., Gomis, M. I., Matthews, J. B. R., Berger, S., Huang, M., Yelekçi, O., Yu, R., Zhou, B., Lonnoy, E., Maycock, T. K., Waterfeld, T., Leitzell, K., Caud, N. (Eds.), Contribution of working group I to the sixth assessment report of the intergovernmental panel on climate change. Cambridge

University Press, Cambridge, pp. 1017.

(18) Oliveira, B. G.; Lourenço, K. S.; Carvalho, J. L. N.; Gonzaga, L. C.; Teixeira, M. C.; Tamara, A. F.; Cantarella, H., Soil pH does not interfere with nitrification inhibitor efficiency for reducing N_2O emissions from soils treated with concentrated vinasse and urea. *Geoderma* **2022**, *426*, 116087.

(19) Fan, D.; He, W.; Smith, W. N.; Drury, C. F.; Jiang, R.; Grant, B. B.; Shi, Y.; Song, D.; Chen, Y.; Wang, X.; He, P.; Zou, G. Global evaluation of inhibitor impacts on ammonia and nitrous oxide emissions from agricultural soils: a meta-analysis. *Glob. Change Biol*. **2022**, *00*, 1-21.

(20) Deng, B.; Fang, H.; Jiang, N.; Feng, W.; Luo, L.; Wang, W.; Wang H.; Hu, D.; Guo, X.; Zhang, L. Biochar is comparable to dicyandiamide in the mitigation of nitrous oxide emissions from *Camellia oleifera* Abel. fields. *Forests* **2019**, *10*, 1076.

(21) Deng, B.; Shen, F.; Guo, X.; Siemann, E.; Zhang, L. Urease inhibitor and biochar independently affected N_2O emissions from *Camellia oleifera* soils. *Plant, Soil Environ.* **2022**, *68*, 424-430.

(22) Zhang, M.; Wang, W.; Tang, L.; Heenan, M.; Xu, Z. Effects of nitrification inhibitor and herbicides on nitrification, nitrite and nitrate consumptions and nitrous oxide emission in an Australian sugarcane soil. *Biol. Fert. Soils* **2018**, *54*, 697-706.

Greenfield, L. M.; Greenfield, L. M.; Graf, M.; Rengaraj, S.; Bargiela, R.; Williams, G.;

(23) Golyshin, P. N.; Chadwick, D. V.; Jones, D. L. Field response of N_2O emissions, microbial communities, soil biochemical processes and winter barley growth to the addition of conventional and biodegradable microplastics. *Agr. Ecosys. Environ.* **2022**, *336*, 108023.

(24) Wang, L.; Hao, D.; Fan, S.; Xie, H.; Bao, X.; Jia, Z.; Wang, L. N_2O emission and nitrification/denitrification bacterial communities in upland black soil under combined effects of early and immediate moisture. *Agriculture* **2022**, *12*, 330.

(25) Xu, X.; Yuan, X.; Zhang, Q.; Wei, Q.; Liu, X.; Deng, W.; Wang, J.; Yang, W.; Deng, B.; Zhang, L. Biochar derived from spent mushroom substrate reduced N_2O emissions with lower water content but increased CH_4 emissions under flooded condition from fertilized soils in *Camellia oleifera* plantations. *Chemosphere* **2022**, *287*, 132110.

(26) Liu H.; Zheng, X.; Li, Y.; Yu, J.; Ding, H.; Sveen, T. R.; Zhang, Y. Soil moisture determines nitrous oxide emission and uptake. *Sci. Total Environ.* **2022**, *822*, 153566.

(27) Puttanna, K.; Gowda, N. M. N.; Rao, E. V. S. P. Effect of concentration, temperature, moisture, liming and organic matter on the efficacy of the nitrification inhibitors benzotriazole, *o*-nitrophenol, m-nitroaniline and dicyandiamide. *Nutr. Cycl. Agroecosys.* **1999**, *54*, 251-257.

(28) Li, H.; Yang, Y.; Hu, Y.; Chen, C.; Huang, J.; Min, J., Dai, L.; Guo, R. Structural analysis and engineering of aldo-keto reductase from glyphosate-resistant *Echinochloa colona*. *J. Hazard. Mater.* **2022**, *436*, 129191.

(29) Zheng, Q.; Wang, W.; Wen, J.; Wu, R.; Wu, J.; Zhang, W.; Zhang, M. Non-additive effects of bamboo-derived biochar and dicyandiamide on soil greenhouse gas emissions, enzyme activity and bacterial community. *Ind. Crop. Prod.* **2023**, *194*, 116385.

(30) Wang, Q.; Fish, J. A.; Gilman, M.; Sun, Y.; Brown, C. T.; Tiedje, J. M.; Cole, J. R. Xander: employing a novel method for efficient gene-targeted metagenomic assembly. *Microbiome* **2015**, *3*, 1-13.

(31) Liu, H.; Yang, X.; Liang, C.; Li, Y.; Qiao, L.; Ai, Z.; Xue, S.; Liu, G. Interactive effects of microplastics and glyphosate on the dynamics of soil dissolved organic matter in a Chinese loess soil. *Catena* **2019**, *182*, 104177.

(32) Rossi, F.; Carles, L.; Donnadieu, F.; Batisson, I.; Artigas, J. Glyphosate-degrading behavior of five bacterial strains isolated from stream biofilms. *J. Hazard. Mater.* **2021**, *420*, 126651.

(33) Manassero, A.; Passalia, C.; Negro, A. C.; Cassano, A. E.; Zalazar, C. S. Glyphosate degradation in water employing the H_2O_2/UVC process. *Water Res.* **2010**, *44*, 3875-3882.

(34) Gimsing, A. L.; Borggaard, O. K.; Jacobasen, O. S.; Aamand, J.; Sørensen, J. Chemical and microbiological soil characteristics controlling glyphosate mineralisation in Danish surface soils. *Appl. Soil Ecol.* **2004**, *27*, 233-242.

(35) Carles, L.; Artigas, J. Interaction between glyphosate and dissolved phosphorus on bacterial and eukaryotic communities from river biofilms. *Sci. Total Environ.* **2020**, *719*, 137463.

(36) Shi, X.; Hu, H.; Kelly, K.; Chen, D.; He, J.; Suter, H.; Response of ammonia oxidizers and denitrifiers to repeated applications of a nitrification inhibitor and a urease inhibitor in two pasture soils. *J. Soil. Sediment.* **2017**, *17*, 974-984.

(37) Menéndez, S., Barrena, I.; Setien, I.; González-Murua, C.; Estavillo, J. M. Efficiency of nitrification inhibitor DMPP to reduce nitrous oxide emissions under different temperature and moisture conditions. *Soil Biol. Biochem.* **2012**, *53*, 82-89.

(38) Menéndez, S.; Merino, P.; Pinto, M.; González-Murua, C.; Estavillo, J. M. Effect of N-(*n*-butyl) thiophosphoric triamide and 3,4 dimethylpyrazole phosphate on gaseous emissions from grasslands under different soil water contents. *J. Environ. Qual.* **2009**, *38*, 27e35.

(39) Chen, Z.; Li, Y.; Xu, Y.; Lam, S. K.; Xia, L.; Zhang, N.; Castellano, M. J.; Ding, W. Spring thaw pulses decrease annual N_2O emissions reductions by nitrification inhibitors from a seasonally frozen cropland. *Geoderma* **2021**, *403*, 115310.

(40) Wang, X.; Bai, J.; Xie, T.; Wang, W.; Zhang, G.; Yin, S.; Wang, D. Effects of biological nitrification inhibitors on nitrogen use efficiency and greenhouse gas emissions in agricultural soils: a review. *Sci. Total Environ.* **2021**, *220*, 112338.

(41) Ren, B.; Huang, Z.; Liu, P.; Zhao, B.; Zhang, J. Urea ammonium nitrate solution combined with urease and nitrification inhibitors jointly mitigate NH_3 and N_2O emissions and improves nitrogen efficiency of summer maize under fertigation. *Field Crop. Res.* **2023**, *296*, 108909.

(42) Park, M. K.; Myers, R. A; Marzella, L. Oxygen tensions and infections: modulation of microbial growth, activity of antimicrobial agents, and immunologic responses. *Clin. Infect. Dis.* **1992**, *14*, 720-740.

(43) Yang, Y.; Hu, Y.; Wang, Z.; Zeng, Z. Variations of the nirS-, nirK-, and nosZ-denitrifying bacterial communities in a northern Chinese soil as affected by different long-term irrigation regimes. *Environ. Sci. Pollut. Res.* **2018**, *25*, 14057-14067.

(44) Jones, C. M.; Spor, A.; Brennan, F. P.; Breuil, M. C.; Bru, D.; Lemanceau, P.; Griffiths, B.; Hallin, S.; Philippot, L. Recently identified microbial guild mediates soil N_2O sink capacity. *Nat. Clim. Change* **2014**, *4*, 801-805.

(45) Park, J. H.; Shin, H. S.; Lee, I. S.; Nae, J. H. Denitrification of high NO_3^--N containing wastewater using elemental sulfur; nitrogen loading rate and N_2O production. *Environ. Technol.* **2002**, *23*, 53-65.

(46) Blum, J. M.; Su, Q.; Ma, Y.; Valverde-Pérez, B.; Domingo-Félez, C.; Mark Jensen, M. M.; Smets, B. F. The pH dependency of N-converting enzymatic processes, pathways and microbes: effect on net N_2O production. *Environ. Microbiol.* **2018**, *20*, 1623-1640.

(47) Lan, Z.; Chen, C.; Rashti, M. R.; Yang, H.; Zhang, D. Stoichiometric ratio of dissolved organic carbon to nitrate regulates nitrous oxide emission from the biochar-amended soils. *Sci. Total Environ.* **2017**, *576*, 559-571.

(48) Zhang, K.; Qiu, Y.; Zhao, Y.; Wang, S.; Deng, J.; Chen, M.; Xu, X.; Wang, Hao.; Bai, T.; He, T.; Zhang, Y.; Chen, H.; Wang, Y.; Hu, S. Moderate precipitation reduction enhances nitrogen cycling and soil nitrous oxide emissions in a semi-arid grassland. *Glob. Change Biol.* **2023**, *00*, 1-16.

(49) Giessen, T. W.; Silver, P. A. Widespread distribution of encapsulin nanocompartments reveals functional diversity. *Nature* 2017, 2, 1-11.

(50) Anderson, C. R.; Peterson, M. E.; Frampton, R. A.; Bulman, S. R.; Keenan, S.; Curtin, D. Rapid increases in soil pH solubilise organic matter, dramatically increase denitrification potential and strongly stimulate microorganisms from the *Firmicutes* phylum. *PeerJ* **2018**, *6*, e6090.

(51) Kits, K. D.; Jung, M.; Vierheiling, J.; Pjevac, P.; Sedlacek, C. J.; Liu, S.; Herbold, C.; Stein, L. Y.; Richter, A.; Wissel, H.; Brüggemann, N.; Wagner, M.; Daims, H. Low yield and abiotic origin of N_2O formed by the complete nitrifier *Nitrospira inopinata*. *Nat. Comm.* **2019**, *10*, 1836.

(52) Pishgar, R.; Dominic, J. A.; Sheng, Z., Tay, J. H.; Denitrification performance and microbial versatility in response to different selection pressures. *Bioresour. Technol.* **2019**, *281*, 72-83.

(53) Schwartz, S. L.; Momper, L.; Rangel, L. T.; Magnabosco, C.; Amend, J. P.; Fournier, G. P. Novel nitrite reductase domain structure suggests a chimeric denitrification repertoire in the phylum *Chloroflexi*. *MicrobiologyOpen* **2022**, *11*, e1258.

Figure Captions

Fig. 1 Impacts of N cycling inhibitor applications on soil (a) glyphosate residues and (b) cumulative N_2O emissions. Lowercase letters indicated significant differences among the different treatments, and capital letters indicated significant differences between the 60% and the 90% WHC in the same treatment. CK, the blank control; DMP, DMPP application; DCP, DCD application; NBP, NBPT application.

Fig. 2 Impacts of N cycling inhibitor applications on soil glyphosate degradation related genes. Lowercase letters indicated significant differences among the different treatments, and capital letters indicated significant differences between the 60% and the 90% WHC in the same treatment. CK, the blank control; DMP, DMPP application; DCP, DCD application; NBP, NBPT application.

Fig. 3 Impacts of N cycling inhibitor applications on soil N-cycling related genes. Lowercase letters indicated significant differences among the different treatments, and capital letters indicated significant differences between the 60% and the 90% WHC in the same treatment. CK, the blank control; DMP, DMPP application; DCP, DCD application; NBP, NBPT application.

Fig. 4 Redundancy analyses revealing the comprehensive linkages among soil chemical properties, 28th N_2O emission rates, glyphosate residues and microbial taxonomic distribution at the phylum level at (a) the 60% WHC and (b) the 90% WHC.

Fig. 5 Pearson's correlation analyses revealing the connections among soil properties, N-cycling related microbes and genes and 28th N_2O emission rates at (a) the 60% WHC and (b) the 90% WHC, and glyphosate degradation related microbes and genes, and glyphosate residues (c) the 60% WHC and (d) the 90% WHC. Solid red arrowhead and red circles indicated positive relationships, and soil bule arrowhead and blue circles indicated negative relationships.

Fig. 6 Pathway analysis revealing the comprehensive linkages among soil properties, 28th N_2O emission rates, glyphosate residues, N-cycling related genes, glyphosate degradation related genes and microbial community structures. Solid red circles indicated positive relationships. soil bule arrowhead indicated negative relationships. Solid red circles indicated no significant relationships between two variables. The significant differences were accepted at $^{*}P < 0.05$, $^{**}P < 0.01$, $^{***}P < 0.001$.

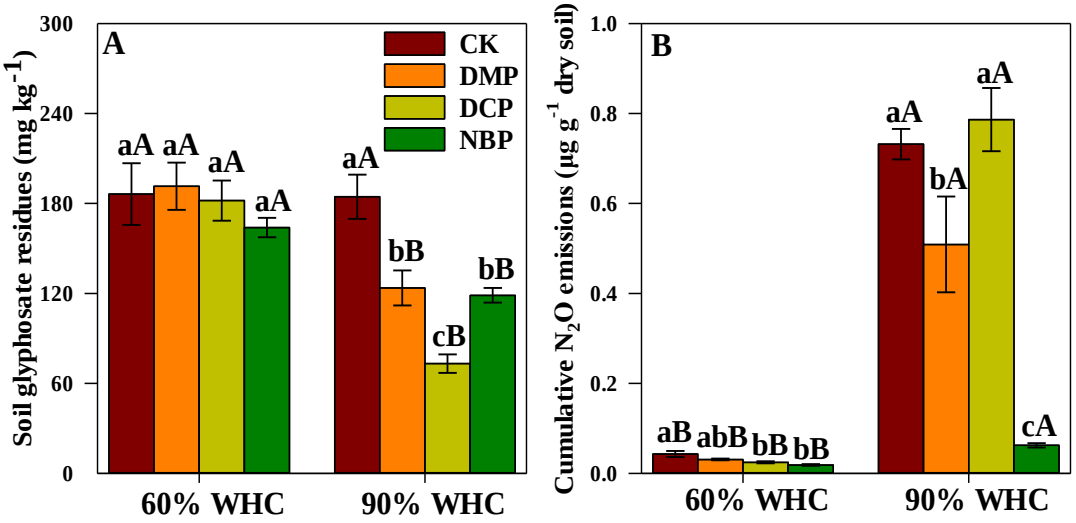

Fig. 1 Impacts of N cycling inhibitor applications on soil (a) glyphosate residues and (b) cumulative N_2O emissions. Lowercase letters indicated significant differences among the different treatments, and capital letters indicated significant differences between the 60% WHC and the 90% WHC in the same treatment. CK, the blank control; DMP, DMPP application; DCP, DCD application; NBP, NBPT application.

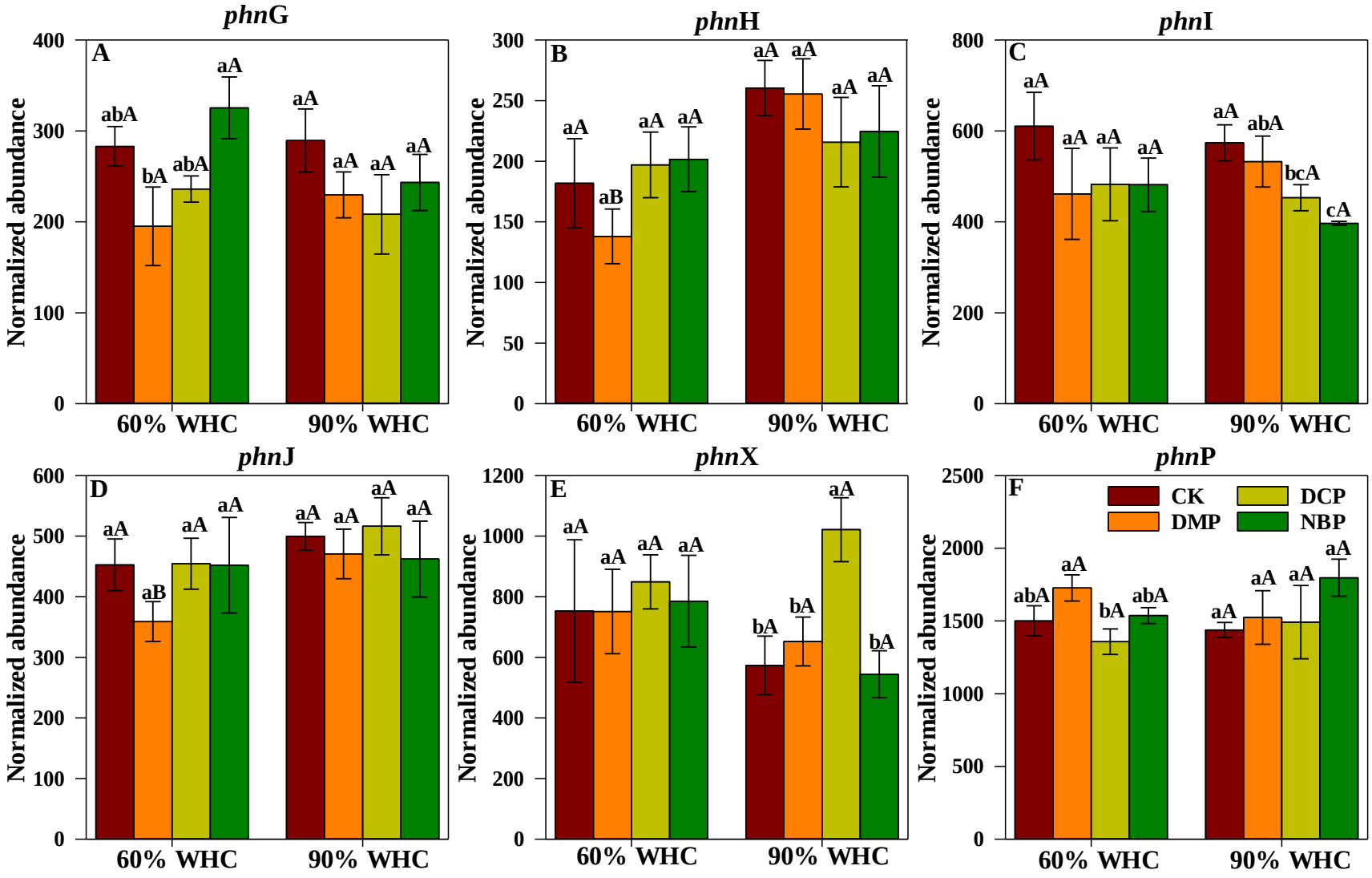
phnG
A
Normalized abundance
400
300
200
100
0
abA
bA
abA
aA
aA
aA
aA
aA
60% WHC
90% WHC
phnH
B
300
250
200
150
100
50
0
aA
aB
aA
aA
aA
aA
aA
aA
60% WHC
90% WHC
phnI
C
800
600
400
200
0
aA
aA
aA
aA
aA
abA
bcA
cA
60% WHC
90% WHC
phnJ
D
600
500
400
300
200
100
0
aA
aB
aA
aA
aA
aA
aA
60% WHC
90% WHC
phnX
E
1200
1000
800
600
400
200
0
aA
aA
aA
aA
bA
bA
aA
bA
60% WHC
90% WHC
phnP
F
2500
2000
1500
1000
500
0
CK
DMP
DCP
NBP
abA
aA
bA
abA
aA
aA
aA
aA
60% WHC
90% WHC

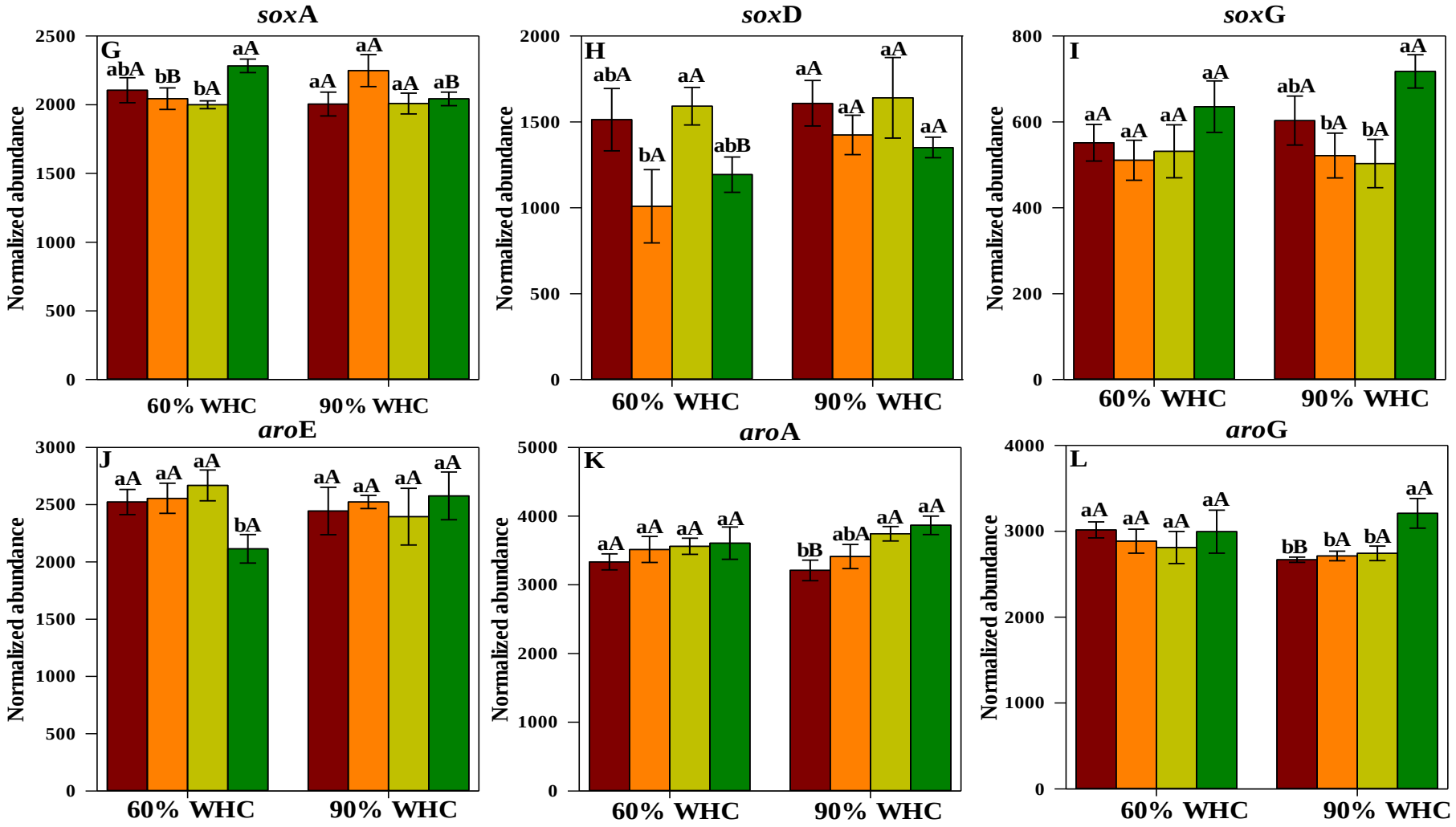

Fig. 2 Impacts of N cycling inhibitor applications on soil glyphosate degradation related genes. Lowercase letters indicated significant differences among the different treatments, and capital letters indicated significant differences between the 60% and the 90% WHC in the same treatment. CK, the blank control; DMP, DMPP application; DCP, DCD application; NBP, NBPT application.

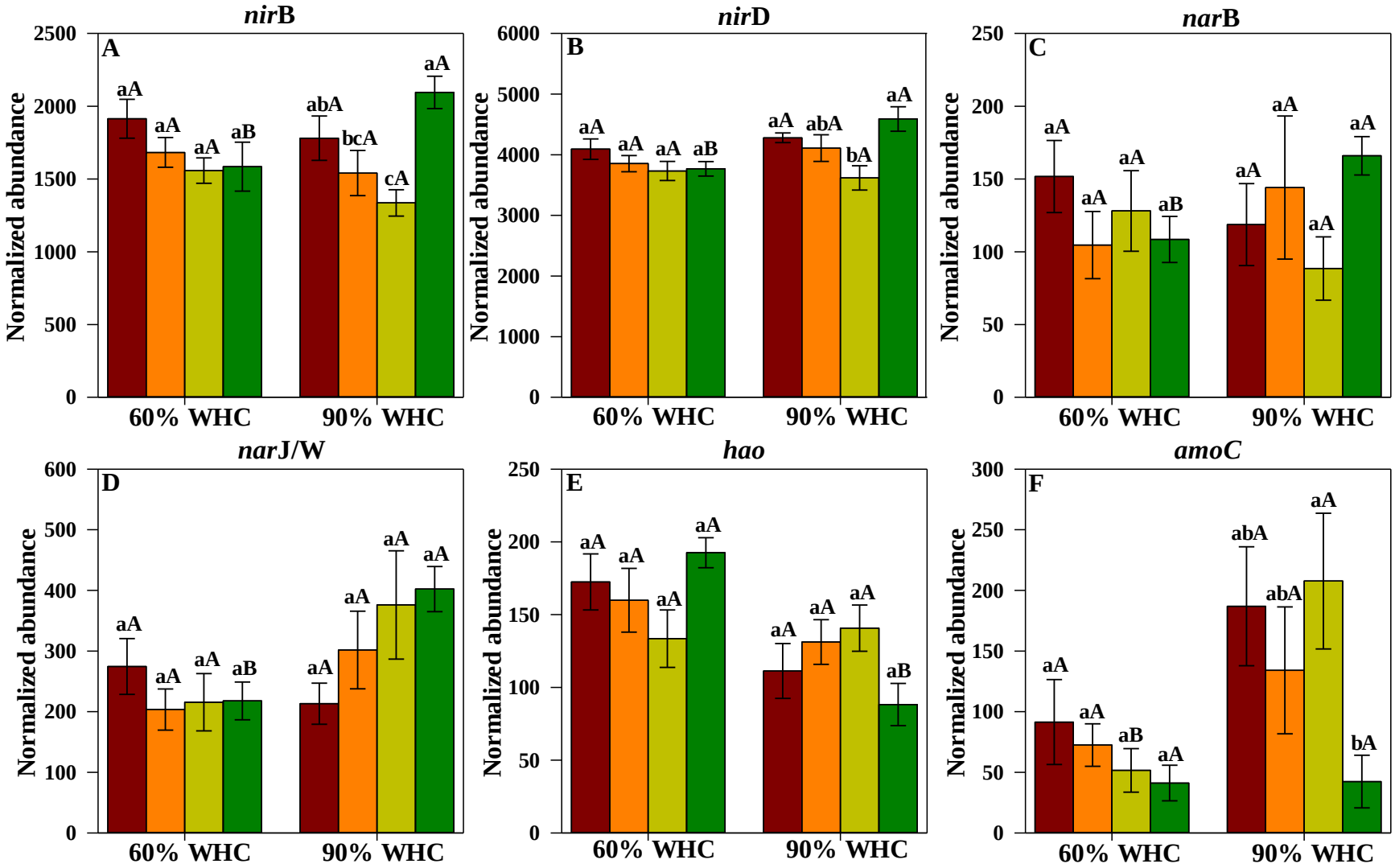
nirB
A
Normalized abundance
2500
2000
1500
1000
500
0
aA
aA
aA
aB
abA
bcA
cA
aA
60% WHC
90% WHC
nirD
B
6000
5000
4000
3000
2000
1000
0
aA
aA
aA
aB
aA
abA
bA
aA
narB
C
250
200
150
100
50
0
narJ/W
D
600
500
400
300
200
100
0
hao
E
amoC
F
300
250
200
150
100
50
0

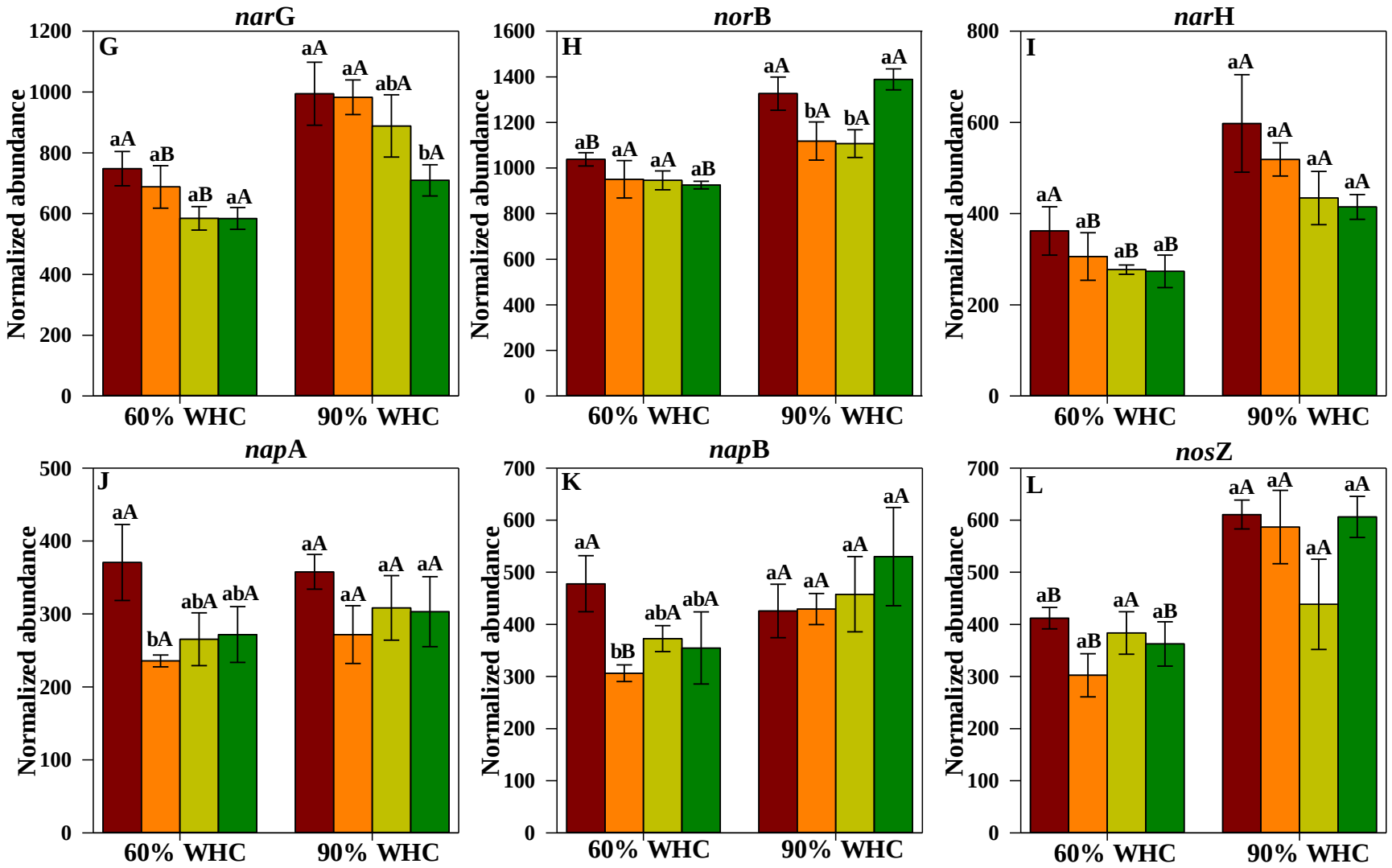
narG
G
Normalized abundance
1200
1000
800
600
400
200
0
aA
aB
aB
aA
aA
aA
abA
bA
60% WHC
90% WHC
norB
H
Normalized abundance
1600
1400
1200
1000
800
600
400
200
0
aB
aA
aA
aB
aA
bA
bA
aA
60% WHC
90% WHC
narH
I
Normalized abundance
800
600
400
200
0
aA
aB
aB
aB
aA
aA
aA
aA
60% WHC
90% WHC
napA
J
Normalized abundance
500
400
300
200
100
0
aA
bA
abA
abA
aA
aA
aA
aA
60% WHC
90% WHC
napB
K
Normalized abundance
700
600
500
400
300
200
100
0
aA
bB
abA
abA
aA
aA
aA
aA
60% WHC
90% WHC
nosZ
L
Normalized abundance
700
600
500
400
300
200
100
0
aB
aB
aA
aB
aA
aA
aA
aA
60% WHC
90% WHC

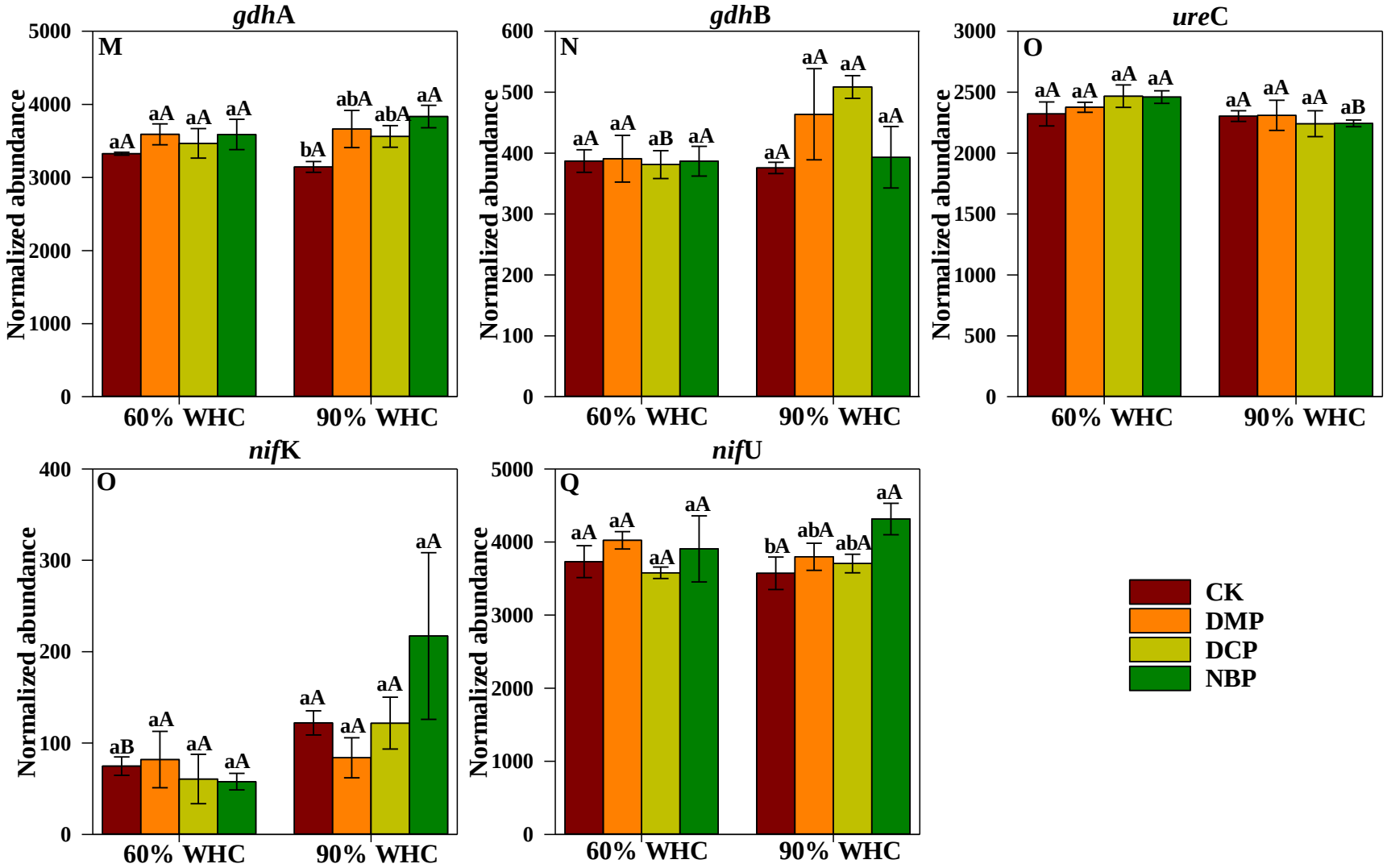

Fig. 3 Impacts of N cycling inhibitor applications on soil N-cycling related genes. Lowercase letters indicated significant differences among the different treatments, and capital letters indicated significant differences between the 60% WHC and the 90% WHC in the same treatment. CK, the blank c

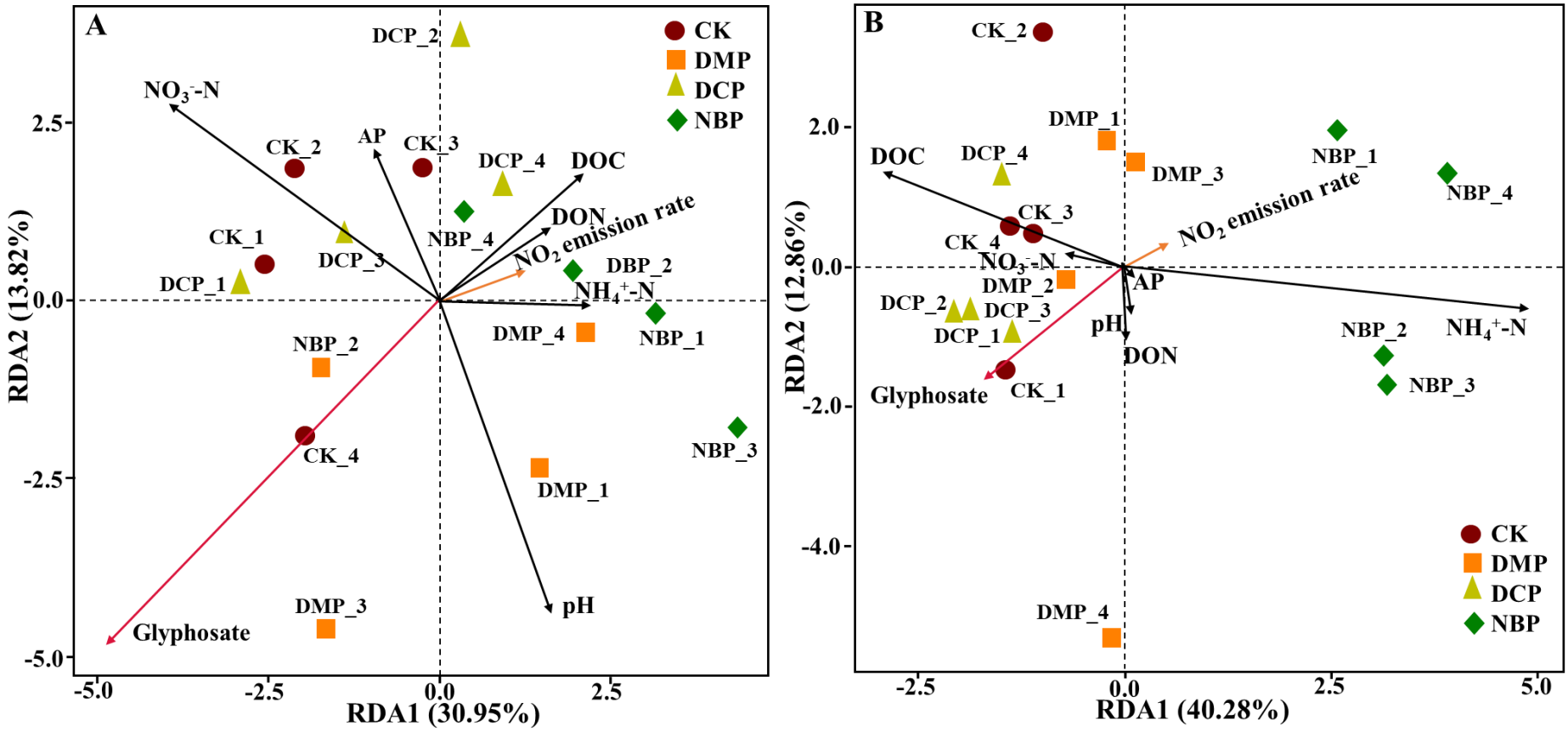

Fig. 4 Redundancy analyses revealing the comprehensive linkages among soil chemical properties, 28th N_2O emission rates, glyphosate residues and microbial taxonomic distribution at the phylum level at (a) the 60% WHC and (b) the 90% WHC.

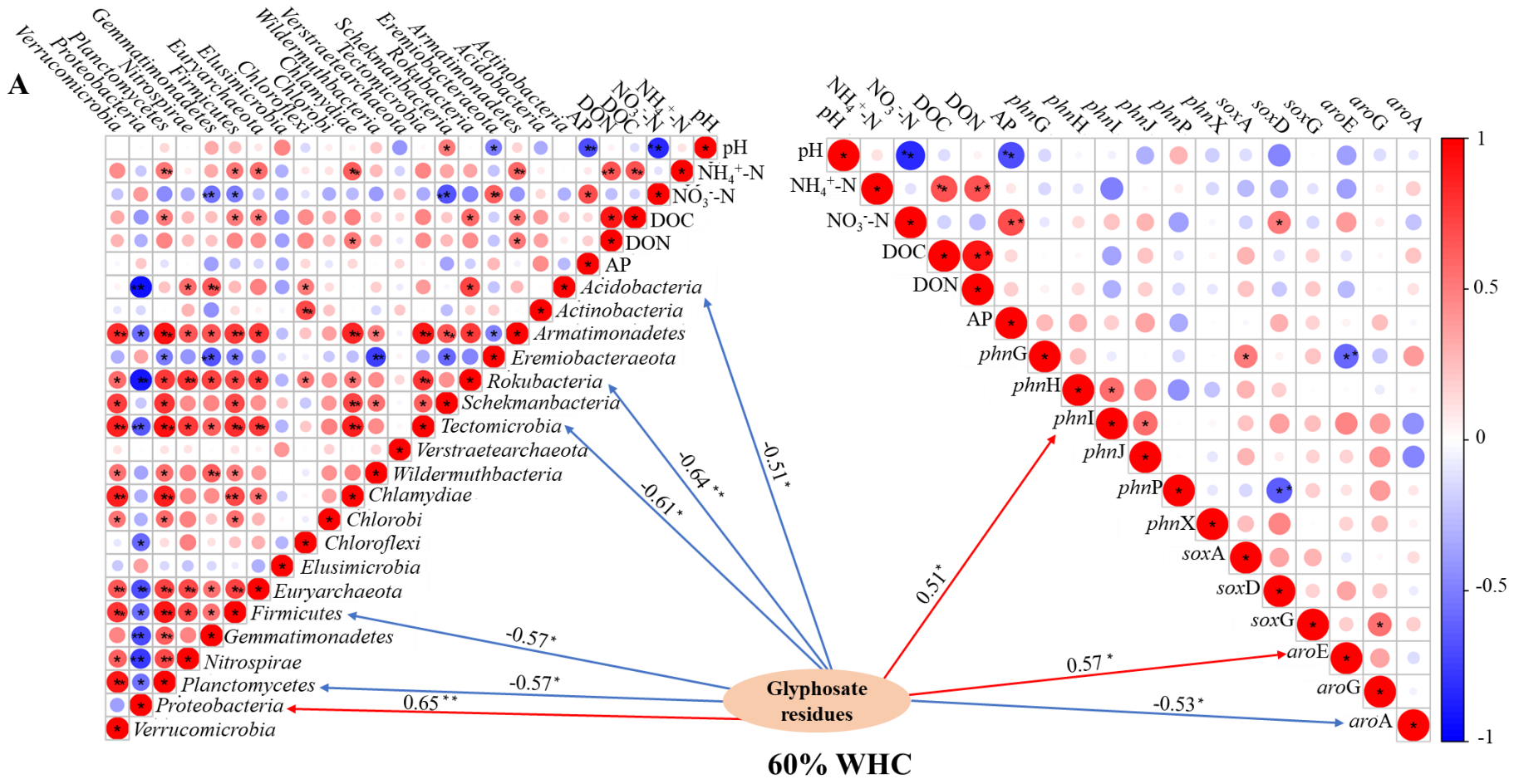
A
Verrucomicrobia
Proteobacteria
Planctomycetes
Nitrospirae
Gemmatimonadetes
Firmicutes
Euryarchaeota
Elusimicrobia
Chloroflexi
Chlorobi
Chlamydiae
Wildermuthbacteria
Verstraetearchaeota
Tectomicrobia
Schekmanbacteria
Rokubacteria
Eremiobacteraeota
Armatimonadetes
Actinobacteria
Acidobacteria
AP
DON
DOC
NO3-N
NH4+-N
pH
phnG
phnH
phnI
phnJ
phnP
phnX
soxA
soxD
soxG
aroE
aroG
aroA
Glyphosate residues
-0.51*
-0.64**
-0.61*
-0.57*
-0.57*
0.65**
0.51*
0.57*
-0.53*
1
0.5
0
-0.5
-1
60% WHC

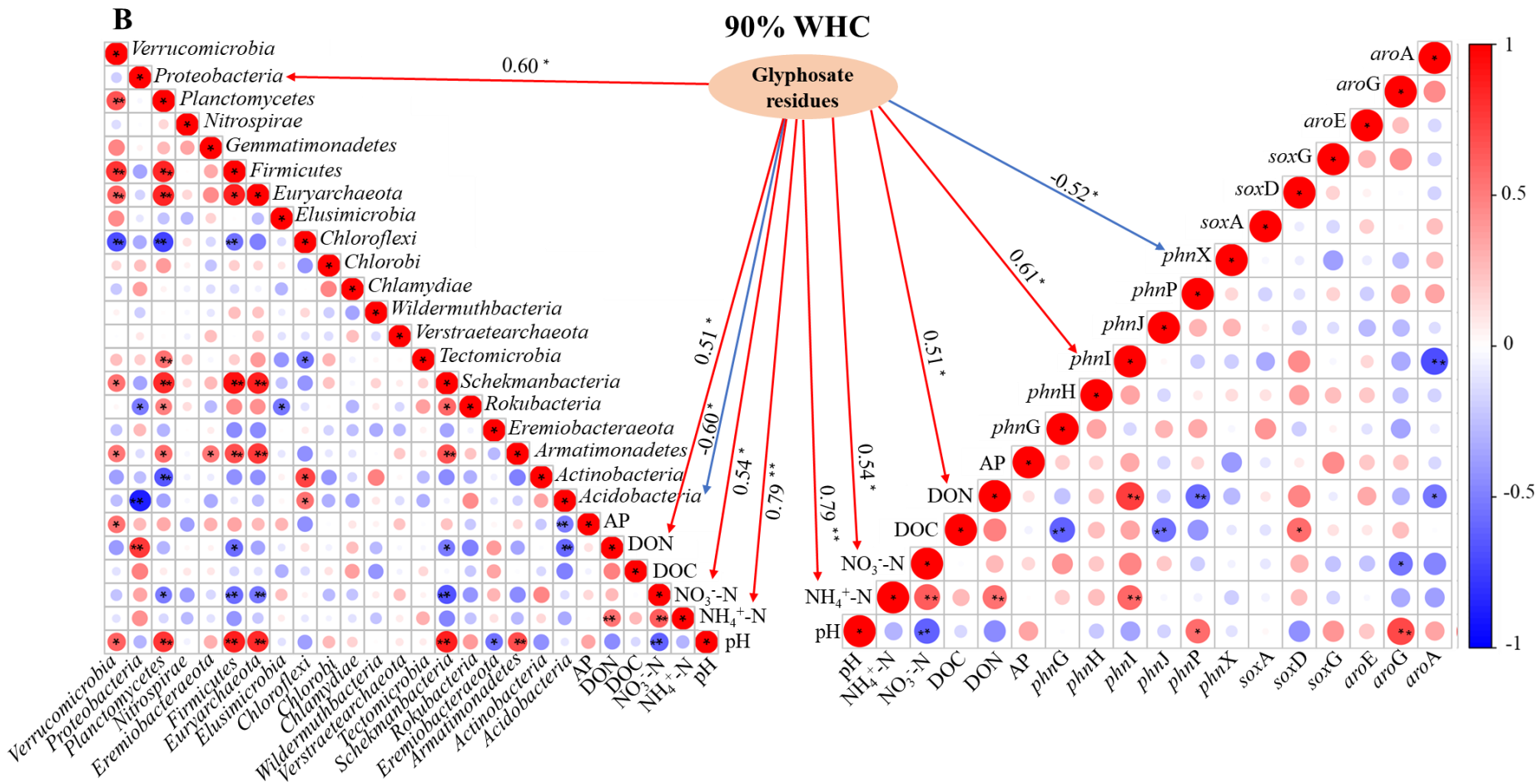
B
90% WHC
Glyphosate residues
0.60 *
0.51 *
-0.60 *
0.54 *
0.79 **
0.79 ***
0.54 *
0.51 *
0.61 *
-0.52 *
Verrucomicrobia
Proteobacteria
Planctomycetes
Nitrospirae
Gemmatimonadetes
Firmicutes
Euryarchaeota
Elusimicrobia
Chloroflexi
Chlorobi
Chlamydiae
Wildermuthbacteria
Verstraetearchaeota
Tectomicrobia
Schekmanbacteria
Rokubacteria
Eremiobacteraeota
Armatimonadetes
Actinobacteria
Acidobacteria
AP
DON
DOC
NO3-N
NH4+-N
pH
aroA
aroG
aroE
soxG
soxD
soxA
phnX
phnP
phnJ
phnI
phnH
phnG
1
0.5
0
-0.5
-1

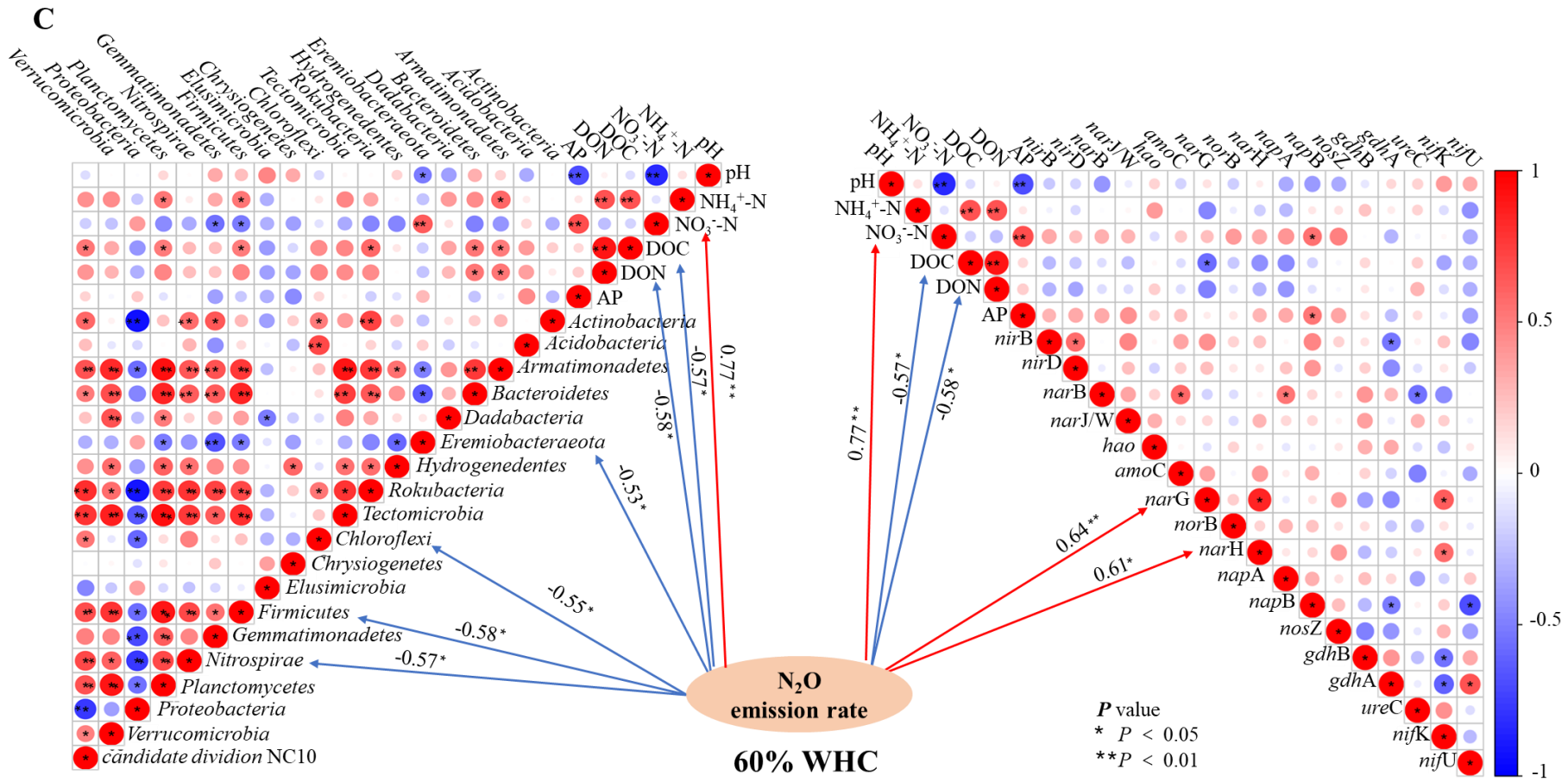
C
Verrucomicrobia
Proteobacteria
Planctomycetes
Nitrospirae
Gemmatimonadetes
Firmicutes
Elusimicrobia
Chrysiogenetes
Chloroflexi
Tectomicrobia
Rokubacteria
Hydrogenedentes
Eremiobacteraeota
Dadabacteria
Bacteroidetes
Armatimonadetes
Acidobacteria
Actinobacteria
AP
DON
DOC
NO3-N
NH4+-N
pH
candidate dividion NC10
-0.55*
-0.58*
-0.57*
-0.53*
-0.58*
-0.57*
0.77**
N2O emission rate
60% WHC
0.77**
-0.57*
-0.58*
0.64**
0.61*
nirB
nirD
narB
narJ/W
hao
amoC
narG
norB
narH
napA
napB
nosZ
gdhB
gdhA
ureC
nifK
nifU
P value
* P < 0.05
**P < 0.01
1
0.5
0
-0.5
-1

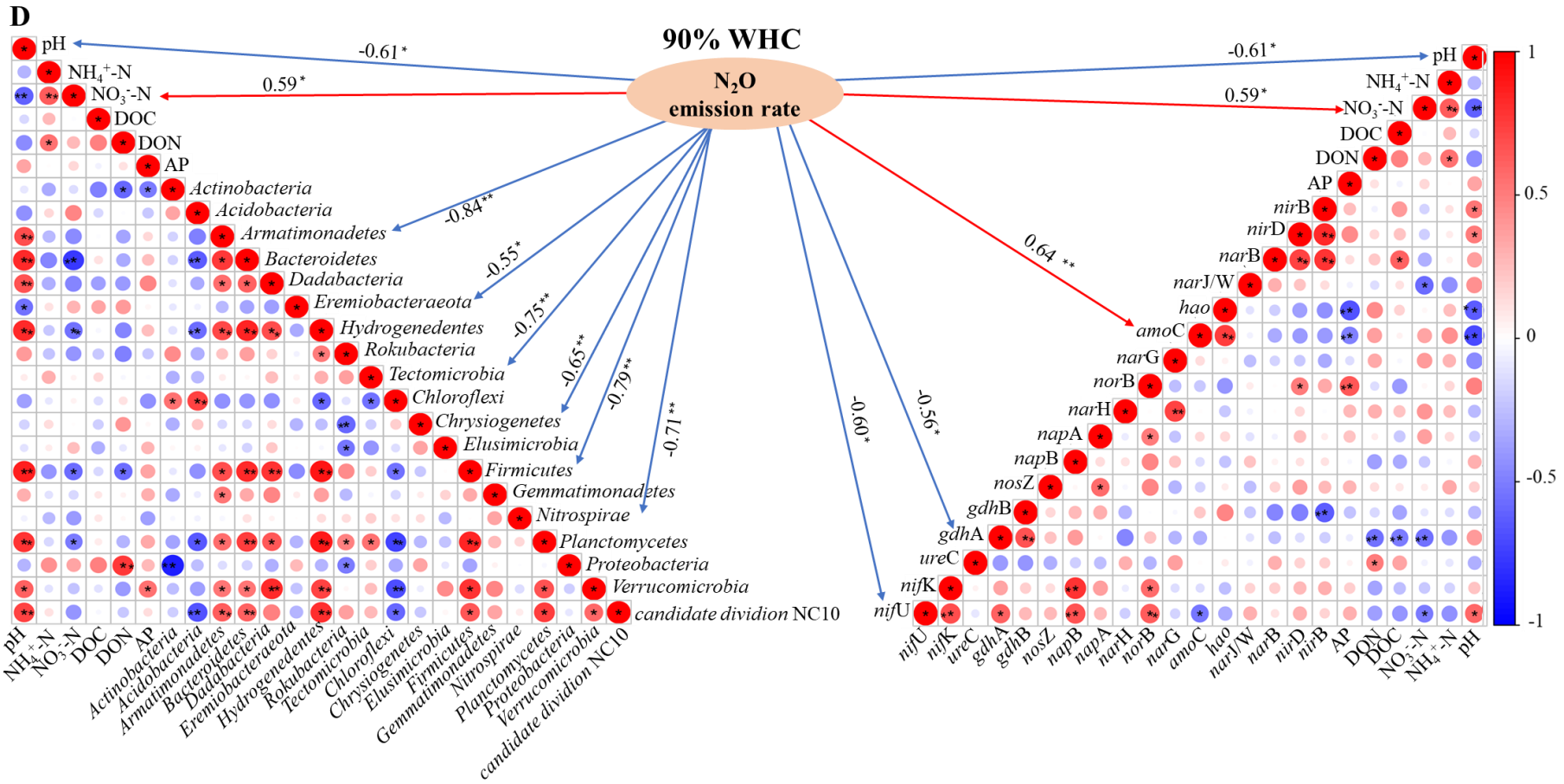

Fig. 5 Pearson's correlation analyses revealing the connections among soil properties, glyphosate degradation related microbes and genes, and glyphosate residues at (a) the 60% WHC and (b) the 90% WHC, and N-cycling related microbes and genes and 28th N_2O emission rates at (c) the 60% WHC and (d) the 90% WHC. Solid red arrowhead and red circles indicated positive relationships, and soil bule arrowhead and blue circles indicated negative relationships.

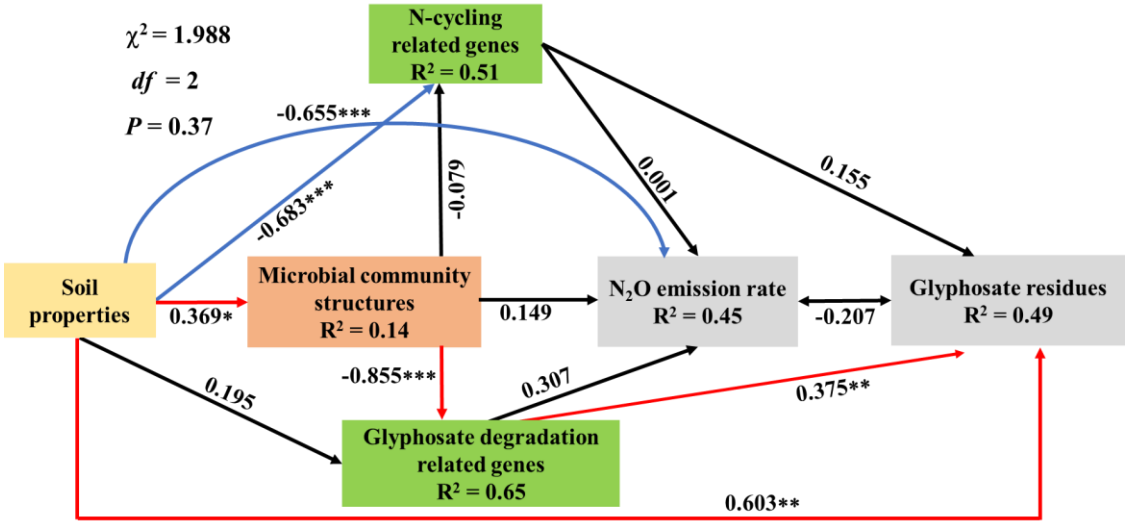

Fig. 6 Pathway analysis revealing the comprehensive linkages among soil properties, 28th N_2O emission rates, glyphosate residues, N-cycling related genes, glyphosate degradation related genes and microbial community structures. Solid red circles indicated positive relationships. soil bule arrowhead indicated negative relationships. Solid red circles indicated no significant relationships between two variables. The significant differences were accepted at $^{*}P < 0.05$, $^{**}P < 0.01$, $^{***}P < 0.001$.

Table Captions

Table 1 Effects of N cycling inhibitors and WHC on soil chemical properties.

Table 1 Effects of N cycling inhibitors and WHC on soil chemical properties.

Factors		pH	DOC mg kg^{-1}	DON mg kg^{-1}	NH_4^+-N mg kg^{-1}	NO_3^--N mg kg^{-1}	AP mg kg^{-1}
60%	CK	.13±0.01bB	103.29±6.57bA	5.64±1.44cA	164.95±14.28aA	20.15±1.54aA	3.53±0.43aA
	DMP	4.72±0.11aB	123.67±9.25bA	12.60±0.76bA	184.50±17.13aA	8.08±0.69bA	1.56±0.16bA
	DCP	4.09±0.11bB	178.52±12.38aA	14.88±0.94bA	200.72±14.16aA	17.52±1.09aA	3.02±0.03aA
	NBP	4.61±0.07aB	169.72±12.38aA	16.73±1.51aA	207.13±12.67aA	7.50±0.20bA	2.79±0.32aA
90%	CK	5.33±0.03bA	98.06±25.79aA	4.08±0.58aA	39.62±9.88aB	1.39±0.10aB	3.51±0.70aA
	DMP	5.44±0.06bA	97.05±17.66aA	3.76±0.22abB	20.67±2.82bB	0.38±0.05cB	2.29±0.65aA
	DCP	5.32±0.07bA	92.99±25.85aB	3.32±0.54abB	17.10±1.42bB	0.62±0.08bB	1.87±0.21aB
	NBP	5.79±0.06aA	91.72±9.81aB	2.68±0.13bB	15.18±0.61bB	0.10±0.01dB	3.28±0.51aA

CK, the blank control; DMP, DMPP application; DCP, DCD application; NBP, NBPT application.